SUPPLEMENTARY INFORMATION

Table of Contents

Victor Sans, Luzian Porwol, Vincenza Dragone, Leroy Cronin*

*WestCHEM, School of Chemistry, The University of Glasgow, Glasgow, G12 8QQ, UK
Email: L.Cronin@chem.gla.ac.uk; website: http://www.croninlab.com

1. General materials and methods

All chemicals were purchased from Sigma-Aldrich and used as received. Solutions were freshly prepared before each experiment.

Once a day, before starting the experiments, a mixture 9:1 D_2O:H_2O was flushed through the cell and the shimming sequence was run to finely tune the apparatus. A Shim sequence is automatically run by Spinsolve software, and when the criteria outlined in Table S1 are met or exceeded, the system is ready to be employed. The machine works on a lock-free basis and therefore can be employed with normal organic, aqueous and fluorinated solvents.

Table S1 Typical values for shimming of Spinsolve

Field	**Value**
Linewidth 50%	< 1 Hz
Linewidth 0.55%	< 40 Hz
SNR	10,000
Signal	ca. 33,000
Noise	Ca. 3.3

Control high field NMR experiments were done employing standard 5 mm NMR tubes and deuterated solvents.

The upper limit in terms of flow rate was calculated taking into account:

- 6 seconds (acquisition time) of residence time in the detector window (5 mm). This should ensure the same package of fluid is in the detection area during a measurement. Applied to a 5 mm. flow cell this implies the upper limit in flow rate is ca. 1 mL min^{-1}.

- 3*T1 seconds in the magnetization coil before reaching the detector. For organic molecules this value typically varies between 2 and 10 s. Therefore applying the upper limit, 45 s. are necessary to ensure full magnetization of the molecules. In a 5 mm. cell this implies the upper flow rate is >10 mL min^{-1}, which is an order of magnitude above what we employed in this work.

2. Details of the experimental set-up

A set of programmable syringe pumps (C3000 Tricontinent) were employed to flow the solutions through the system. The pumps are controlled employing in-house developed LabView applications. The reactors employed are based on different lengths of tubing of 1/8“ OD (1.5 mm ID) made in Polytetrafluoroethylene (PTFE). The mixers are based on 1/8“ 4-way and 6-way mixers made in PTFE. Standard fittings were employed to connect the different parts.

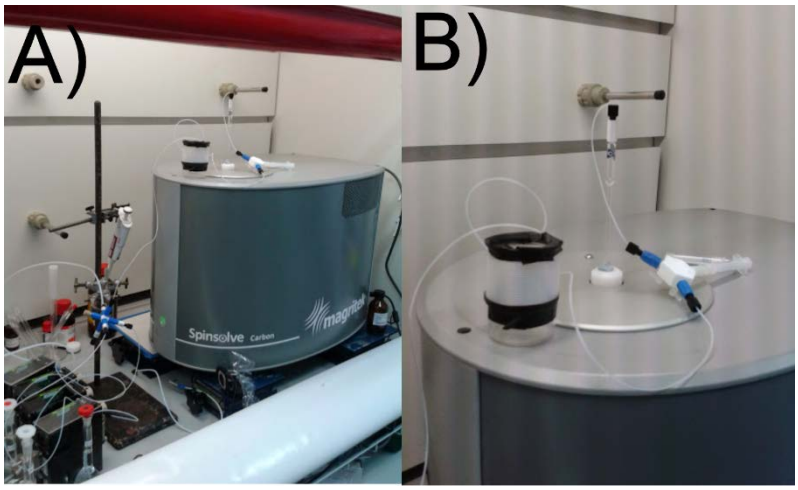

Fig. S1 Experimental rig employed in this work.

An in-house developed flow cell (Fig. S2) was employed to maximise the sensitivity from the measurements. The cell was made by cutting a 5 mm NMR tube and connecting it to two pieces of glass rod. The upper part of the glass rod was connected to a glass threaded connector from Omnifit. This allowed the employment of standard fittings.

Fig. S2 Detail of the glass flow-cell employed in this work.

3. LabView interface

LabView based interfaces were developed for the different assays performed in this work. They controlled and synchronised the pumps, connected to Spinsolve software via a TCP/IP connection, hanlded and interpreted the NMR data and the feedback algorithm. Fig. S3 shows a snapshot of the main VI.

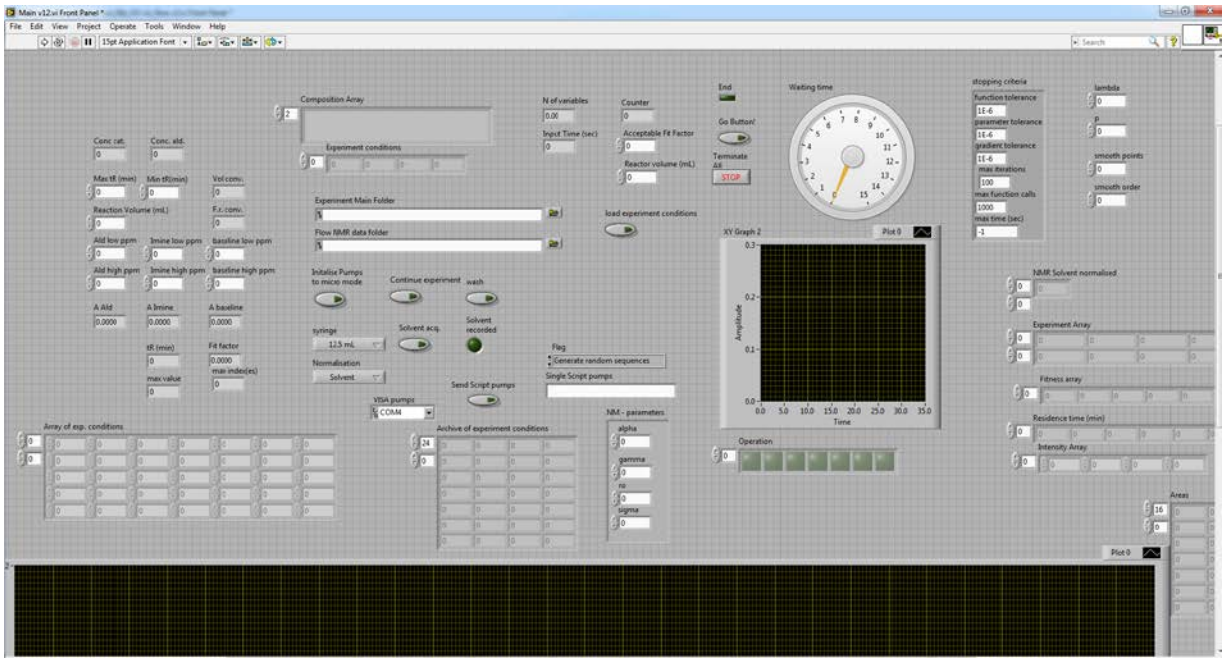

Fig. S3 Snapshot of the main VI programmed to control the Flow-NMR platform.

Spinsolve software allows remote control via TCP/IP connections to a predefined port. Fig. S4 shows a snapshot of a subVI employed to remotely call Spinsolve to start an experiment.

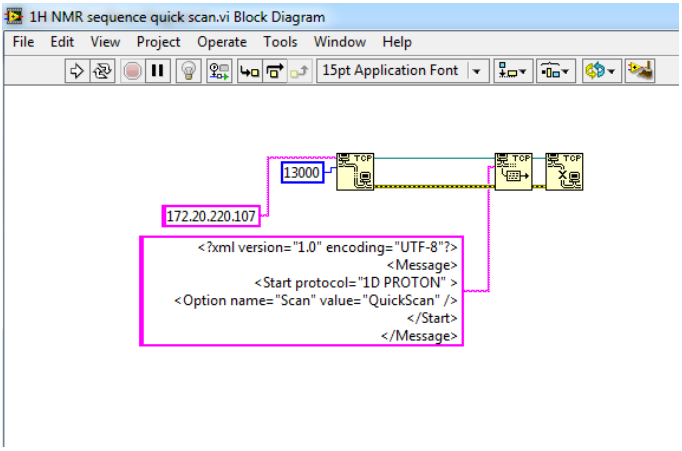

Fig. S4 LabView script to remotely call Spinsolve.

A simplified vi was programmed for the cases where no feedback was needed. In this cases, the program loads a set of predefined sequences, executes them and acquires the required spectra in each sequence, see Fig. S5 for a snapshot.

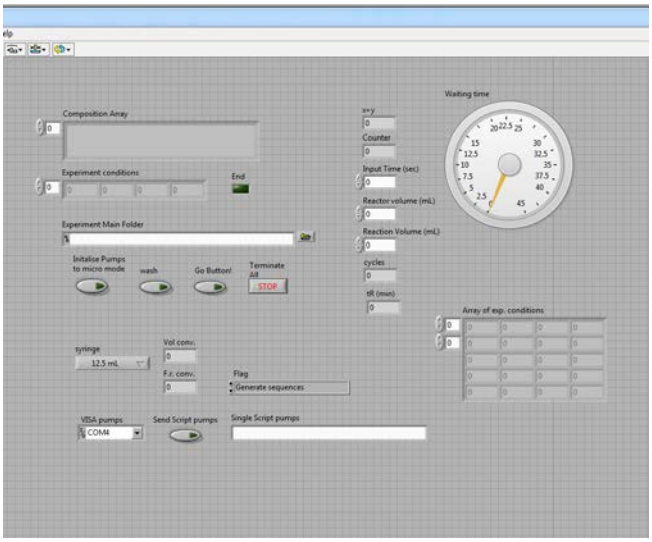

Fig. S5 Simplified VI for the execution of predefined sequences, where no feedback is required.

4. Experimental set-up for the imine synthesis

This case represents a minimalistic set-up for the Flow-NMR. Each of the two reagents was delivered employing a C3000 pump and mixed employing a standard T-junction at the top of the NMR. A 1/8“ tubing connected in a downflow configuration was passed through the NMR chamber and connected in the bottom employing standard fittings. With this configuration, the reactor volume is the length of tube from the top of the reactor until the detection point.

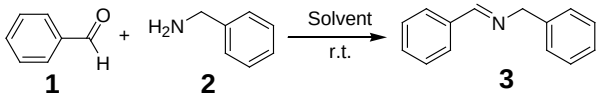

Scheme S1 Imine synthesis employed as benchmark reaction for the Flow-NMR.

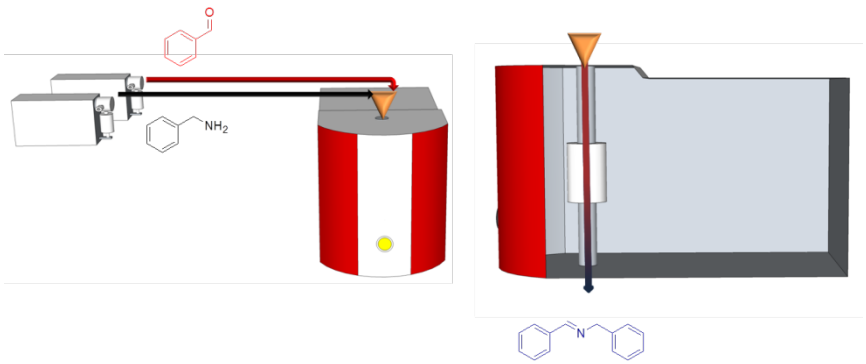

Fig. S6 Schematic of the flow set-up employed for the imine synthesis.

5. DEPT spectra corresponding to the imine synthesis

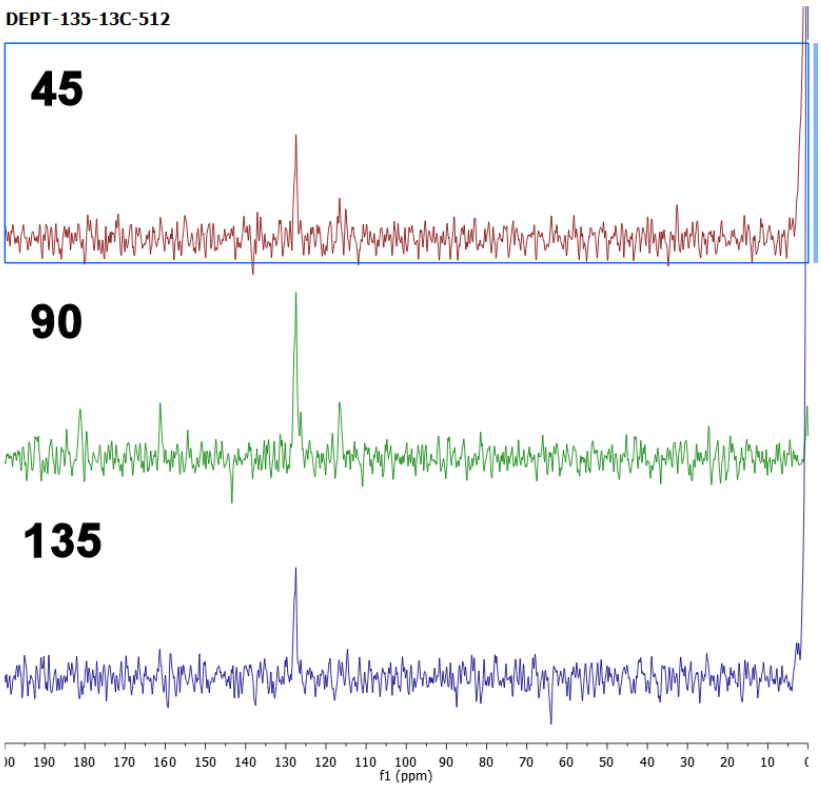

Fig. S7 DEPT 45, 90 and 135 corresponding to the reaction mixture in the imine synthesis between benzaldehyde and benzylamine.

6. Fluorination reactions

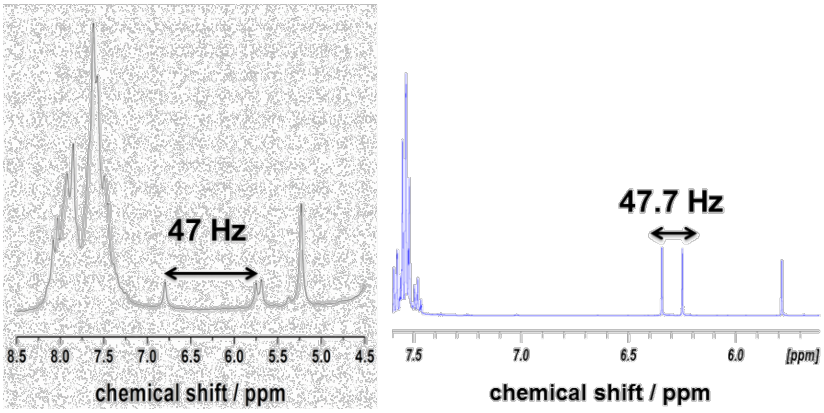

Fig. S8 Comparison of the J coupling observed under flow conditions in Spinsolve and in a 400 MHZ high-field Bruker machine.

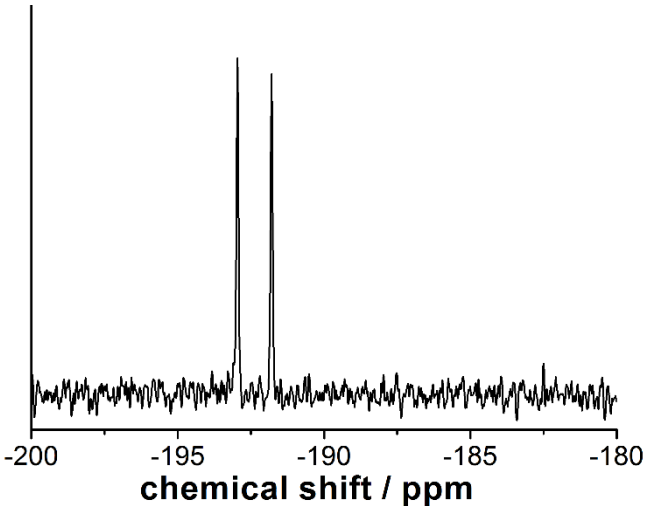

Fig. S9 ^{19}F NMR spectrum of the reaction mixture acquired over a long acquisition time (78 minutes).

7. Monitoring the influence of the catalyst on the Diels-Alder cycloaddition employing in-line flow-NMR

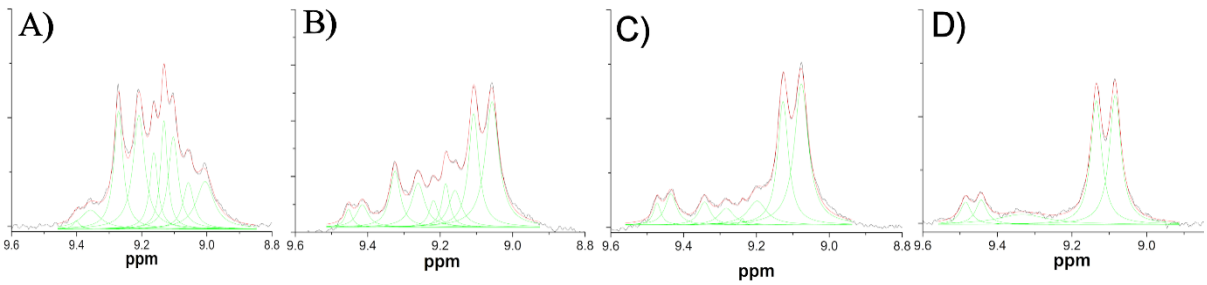

Fig. S10 Spectra corresponding to the Diels-Alder reaction between cyclopentadiene and acrolein catalysed by $Sc(OTf)_3$. A) 0 mol% of catalyst added. B) 0.5 mol%. C) 1 mol%. D) 3 mol %.

8. Self-optimization employing Flow-NMR

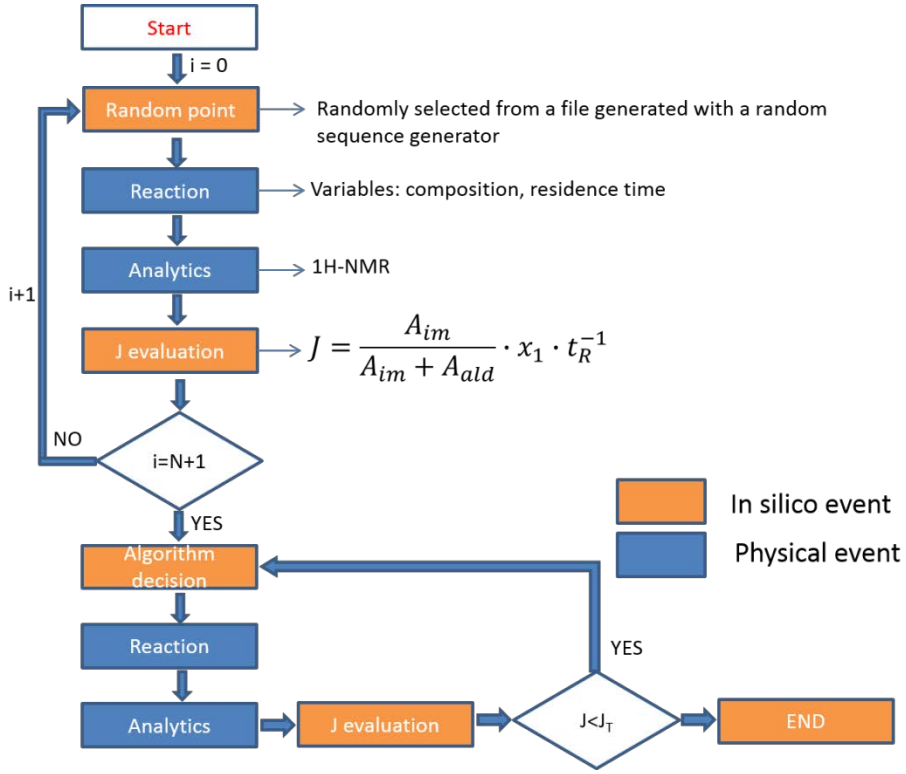

Fig. S11 Scheme of the decision making process for the self-optimization of organic reactions employing Flow-NMR.

The Nelder-Mead algorithm has been described elsewhere.[1] The modifications added in this work respect to the original is the ability of the algorithm to contract the simplex if no improvement is observed and the reduction of the simplex towards the best result if no improvement is obtained through the normal steps (reflection, expansion, contraction, internal contraction).

Table S1 Experimental conditions corresponding to the self-optimization investigated in this work.

Entry	x_1	x_2	x_3	t_R / min	J
0	0.031	0.945	0.024	9.089	0.002
1	0.401	0.416	0.183	5.792	0.068
2	0.226	0.082	0.692	3.093	0.052
3	0.4	0.414	0.185	3.462	0.116
4	0.489	0	0.511	2	0.028
5	0.574	0.426	0	3.077	0.142
6	0.557	0.443	0	3.069	0.021
7	0.575	0.144	0.281	2	0.173
8	0.661	0.008	0.33	2	0.031
9	0.453	0.547	0	4.359	0.093
10	0.518	0.482	0	3.269	0.011
11	0.503	0.164	0.333	2	0.062
12	0.617	0.217	0.166	2	-0.026
13	0.575	0.003	0.422	2	0.016
14	0.662	0.01	0.329	2	0.030
15	0.661	0.244	0.095	2	0.197
16	0.661	0.244	0.095	2	0.206
17	0.659	0.341	0	2	0.054
18	0.574	0.394	0.033	2	0.232
19	0.475	0.525	0	2	0.040
20	0.607	0.393	0	2	0.025
21	0.638	0.356	0.006	2	0.054
22	0.596	0.215	0.189	2	0.175
23	0.575	0.144	0.281	2	0.145
24	0.628	0.32	0.052	2	0.249
25	0.613	0.115	0.272	2	0.122
26	0.622	0.371	0.007	2	0.103
27	0.619	0.268	0.113	2	0.224
28	0.714	0.161	0.125	2	0.168
29	0.58	0.369	0.051	2	0.265
30	0.644	0.175	0.181	2	0.141
31	0.581	0.407	0.011	2	0.114
32	0.606	0.315	0.079	2	0.231

9. References

[1] Nelder, J. A.; Mead, R. *The Computer Journal* **1965**, *7*, 308.